Title:

Genetic risk implicating endolysosomal network genes correlates with endolysosomal dysfunction across neural cell types in Alzheimer's disease

Mamde S*[1], Rose SE*[2], Prater KE*[3], Cochoit A[3], Lin YF[4], Smith I[3], Johnson CS[3], Reid AN[3], Qiu W[4], Strohbehn S[5], Keene CD[2], Lee SI[4], Lin KZ[6], Rolf BA[5], Garden GA[7], Blue EE[5,6], Young JE[#1,9], Jayadev S[#3,5,9]

1. Department of Cellular and Molecular Medicine, University of California San Diego, San Diego, CA.
2. Department of Laboratory Medicine and Pathology, University of Washington, Seattle WA
3. Department of Neurology, University of Washington, Seattle WA
4. Paul G Allen School of Computer Science and Engineering, University of Washington, Seattle WA
5. Department of Medicine, Division Medical Genetics, University of Washington, Seattle WA
6. Brotman Baty Institute, Seattle, WA and Institute for Public Health Genetics, School of Public Health, University of Washington, Seattle, WA
7. Department of Biostatistics, School of Public Health, University of Washington, Seattle WA
8. Department of Neurology, University of North Carolina, Chapell Hill, NC
9. Institute of Stem Cell and Regenerative Medicine, University of Washington, Seattle WA

* authors contributed equally to this work
# co-corresponding authors

Correspondence:
Jessica Young PhD: jeyoung@uw.edu
Suman Jayadev MD: sumie@uw.edu

Funding Sources:
NIA: UW Alzheimer Disease Training Program T32
NIA: P30 AG066509 UW Alzheimer Disease Research Center
NIA: R01AG080585, RF1AG063540

Acknowledgements: We are grateful to study participants and their families for making the generous donation of their brain for research.

The authors have nothing to declare

ABSTRACT

Late-onset Alzheimer's disease (LOAD) has a complex genomic architecture. LOAD risk variants suggest multiple pathways, including the endolysosomal network (ELN), contribute to the pathobiology of Alzheimer's disease (AD). Whether genetic risk in specific pathways correlates with corresponding biological dysfunction remains largely unknown. We developed an endolysosomal pathway-specific polygenic risk score (ePRS) using 14 well-established AD risk alleles implicating ELN genes. We investigated the association between ePRS and AD neuropathology, then examined cell-specific endolysosomal morphology and transcriptomic profiles in post-mortem dorsolateral prefrontal cortex samples from donors stratified by ePRS burden. We found that the ePRS was significantly associated with AD diagnosis and neuropathological measures, comparable to a pathway-agnostic PRS despite representing far fewer loci. High ePRS correlated with increased neuronal endosome volume, number and perinuclear aggregation independent of AD pathology. Single-nucleus RNA sequencing revealed cell type-specific transcriptomic changes associated with ePRS status, influencing glutamatergic signaling, protein homeostasis, responses to DNA damage and immune function. Neurons, astrocytes, oligodendrocytes, and microglia each showed varied gene expression patterns associated with ePRS burden. Together, these results provide evidence that AD genetic risk variants harboring ELN genes correlate with endolysosomal dysfunction in human brain tissue. These findings suggest that pathway-specific genetic risk contributes to corresponding cellular pathology in AD and nominates candidate mechanisms by which ELN AD variants contribute to pathogenesis.

INTRODUCTION

Recent clinical trials targeting amyloid beta removal in late-onset Alzheimer's disease (LOAD) have shown modest potential benefits, yet there is room for more effective interventions. Drug development in AD has been hindered by an incomplete understanding of its mechanisms, largely due to the disease's heterogeneous nature involving multiple biological pathways and cell types. While amyloid beta is present in AD brains and necessary for the development of the AD phenotype, the progressive degeneration leading to cognitive decline results from multiple cellular responses across several disease phases[3]. Elucidating these aspects of disease progression may reveal additional intervention targets.

Genome-Wide Association Studies (GWAS) and candidate gene approaches have revealed the complex genomic architecture underlying LOAD[3-8] by identifying nucleotide polymorphisms (SNPs) tagging discrete regions of chromosomes or loci, associated with AD. Genes within these risk loci have suggested pathogenic clues to etiology; genomic regions correlated to AD may harbor genes relevant to AD pathophysiology. Notably, GWAS of LOAD involve hundreds of thousands of individuals but detailed molecular studies of human brain tissue are not currently feasible at that scale due to limitations in tissue availability and resources. Therefore, human genetic variation presents a significant challenge in investigating LOAD pathogenesis when attempting to derive mechanistic insights from patient samples in a reasonably sized cohort. In this study, we developed approaches to these problems to understand AD pathophysiology that would leverage, rather than be limited by human variation.

The aggregate burden of common genetic variants identified by GWAS is predictive for increased risk for AD at an individual level[10]. Polygenic risk scores (PRS) calculating a weighted cumulative load of AD genetic SNPs predict risk for AD incidence as well as various AD biomarkers, neuropathology and endophenotypes[11-18]. GWAS studies have identified variant haplotypes harboring genes in immune, synaptic function, lipid metabolism, endolysosomal pathways among others[19] nominating those pathways candidate AD drivers. Whether variant burden in one pathway or another, often generated as a pathway specific risk polygenic risk score, actually correlates to observable pathway changes nominated by the variant is largely not known and remains a significant gap in the goal to map the mechanisms linking variant to disease pathogenesis. The endolysosomal network (ELN) plays important cell-type specific roles in brain homeostasis and is already strongly linked to AD pathogenesis[20-22]. However, it is not known if endolysosomal network risk loci contribute to observed ELN pathology in AD, and if they also

confer additional gene regulatory or functional changes relevant to AD pathology. Determining whether or not having a higher burden of ELN risk portends a more likely role for ELN dysfunction could have important implications for future targeted therapies in some individuals.

We hypothesized that a higher burden of ELN risk loci drives endolysosomal pathology and could be observed when compared to AD without high ELN genetic risk burden. In the context of AD pathology we further hypothesized that higher ELN burden results in gene expression profiles distinct from AD without ELN risk. To test our hypotheses, we investigated the correlation of an endolysosomal polygenic risk score (ePRS), representing 13 established AD GWAS loci which contain genes of the endolysosomal network, with cell-type specific cellular and molecular phenotypes in AD and control brain tissue.

RESULTS

Pathway Specific PRS predicts AD status and AD neuropathologic measures

Polygenic risk scores (PRS) combine the effects of many SNPs into a single measure of accumulated risk, and their association with AD risk varies by which variants are included and how their signals are combined [23]. PRS limited to AD GWAS hits implicating genes within specific pathways provide insight into pathogenesis. Endocytosis-focused PRS are associated with risk of AD and mild cognitive impairment [18], AD biomarkers [11, 14, 15], and multiple cognitive measures[11]

We hypothesized that the cumulative burden of ELN-affiliated risk alleles impacts cell type-specific ELN function, thus contributing to LOAD pathogenesis. To test this hypothesis, we first developed an ELN pathway-specific polygenic risk score (ePRS) combining information from 13 AD GWAS SNPs (Table 1) and contrasted it with a pathway-agnostic PRS focused on common AD GWAS hits with relatively strong effect sizes (Table 1 + rs7274581, rs10838725, rs6656401, rs8093731, rs17125944, rs35349669, rs2718058, rs10498633, rs1476679)[4, 24, 25].

Table 1. ePRS variants identified through AD GWAS

rsID	Gene	Odds Ratio	European allele frequency
rs10792832	*PICALM*	0.87	0.3534
rs10948363	*CD2AP*	1.1	0.2671
rs11218343	*SORL1*	0.77	0.03893
rs11771145	*EPHA1*	0.9	0.3606
rs190982	*MEF2C*	0.93	0.3752
rs28834970	*PTK2B*	1.1	0.335
rs4147929	*ABCA7*	1.15	0.171
rs3764650	*ABCA7*	1.37	0.08409
rs3865444	*CD33*	0.94	0.3212
rs670139	*MS4A4E*	1.08	0.4273
rs6733839	*BIN1*	1.22	0.3921
rs744373	*BIN1*	1.24	0.2909
rs9271192	*HLA-DRB1*	1.11	0.276
rs9331896	*CLU*	0.86	0.398

Table 1:
Fourteen variants identified through AD GWAS used to create the ePRS score.

We calculated both PRS in a local sample of clinically and neuropathologically confirmed AD cases and controls and the AD Sequencing Project data (ADSP). We transformed the risk scores into deciles defined by the larger ADSP data set, then tested their association with AD neuropathology after adjusting for sex and *APOE* ε4 carrier status in the UW sample and sex, ε2, ε4, population structure, and relatedness in the ADSP. We found that the significant association between ePRS and multiple AD neuropathology measures in the UW and ADSP samples was comparable to the pathway-agnostic PRS despite representing ~50% of the AD GWAS loci (p-value < 0.05; Figure 1). A one-decile increase in our ePRS was significantly associated increase in ADNC, Braak, CERAD, and Thal stage within the larger ADSP cohort, and was nominally associated with an increase in ADNC, CERAD, and Thal stage within our modest UW cohort.

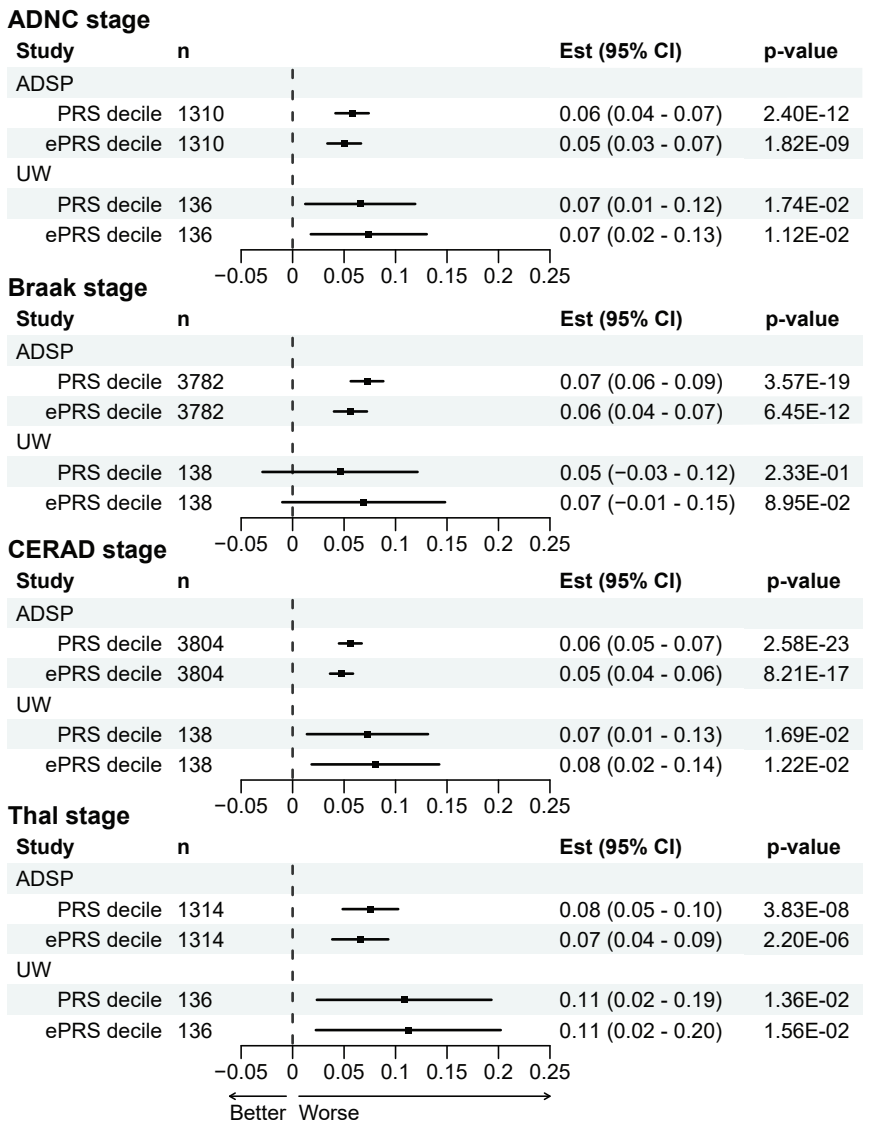

Figure 1:

Association between ePRS, PRS, and AD neuropathology. X-axis: effect size (point) and 95% confidence interval (line) for association with ADNC [1], Braak [2], CERAD [2], and Thal [9] scores. Covariates include sex + ε4 carrier status (UW) or sex, ε2 and ε4 dose, population structure, and relatedness (ADSP).

ePRS is associated with cell type specific endolysosomal cytopathology

The relationship between abnormal and enlarged early endosome pathology and AD is well established in the literature, both in post-mortem brain and model systems[26-29]. We analyzed

early endosomes in neurons from high and low ePRS cases from our tissue cohort (Table 2) using quantitative immunofluorescence and confocal microscopy. Due to the abundance of these organelles in the neurons we analyzed early endosome changes in the somatodendritic and perinuclear neuronal regions separately. Figure 2 A-D shows representative neurons at different ADNC stages (0-3). We observed a higher number of endosomes in neurons with high ePRS (Figure 2E,F), a finding seen in other neurodegenerative disease studies[30], indicative of altered function. Increased perinuclear early endosome aggregation with high ePRS was observed across ADNC levels; for example, the representative AD case with low ePRS in Figure 2C (ADNC 2 regarded as having sufficient pathology to predict dementia per neuropathology consensus guidelines) has smaller and fewer endosomes in the perinuclear region than the high ePRS individual who also has AD pathology (Figure 2D). This observation was true regardless of ADNC level. Interestingly, the high ePRS genetic background was also significantly correlated with enlarged endosome size in the perinuclear region in cases with intermediate to high AD pathology although not in the somatodendritic region (Figure 2E-F, red bars). Perinuclear aggregation of endolysosomes has been observed in LOAD hippocampal neurons[31] and we also noted striking aggregation of early endosomes in the perinuclear region of high ePRS cases with AD pathology (Figure 2G)

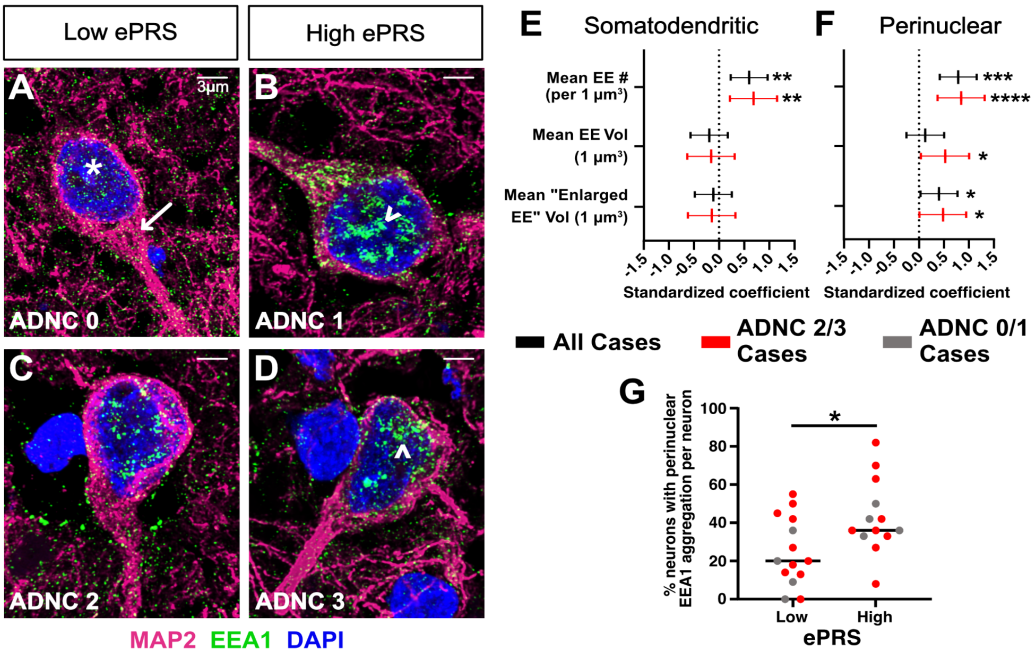

Figure 2:

ePRS shifts the size and number of early endosomes primarily in the perinuclear compartment in post-mortem cortical neurons. A-D) Representative pyramidal neurons from postmortem parietal cortex. MAP2 (magenta) labels somatodendritic region of the neuron compartment, EEA1 (green) labels early endosomes (EEs), and DAPI (blue) labels nuclei. Perinuclear region of interest (ROI) noted with asterisk; somatodendritic ROI noted with arrow. A, C) Neurons from low ePRS cases have minimal EE aggregation in the perinuclear region, shown in both A) no-low AD (ADNC 0/1) and C) AD (ADNC 2/3) cases. B, D) Neurons in high ePRS cases have distinct increase in perinuclear EE aggregation (white arrowheads), shown in both B) no-low AD (ADNC 0/1) and D) AD (ADNC 2/3) cases. E-F) Correlation between ePRS and EE morphology metrics using a linear regression model. E) High ePRS correlates with a significant increase in somatodendritic EE number in the full cohort ("All cases", black). This relationship between increasing ePRS and somatodendritic EE density remained significant even when intermediate-high AD cases only were included in the model ("ADNC 2/3 cases", red). F) High ePRS correlates with a significant increase in perinuclear EE number and size in the full cohort ("All cases", black). When only intermediate-high AD cases were considered in the model, the positive correlation between high ePRS and perinuclear EE number and size becomes more pronounced ("ADNC 2/3 cases", red). G) The percentage of neurons imaged per case with clear perinuclear EE aggregation (neurons assigned yes/no for presence of aggregation) was significantly increased in the high ePRS cases compared to low ePRS. ADNC 2/3 cases in red to show that AD cases are represented in both low and high ePRS groups. Scale bars are 3 µm in all images. *p<0.05, **p<0.01, ***p<0.001, ****p<0.0001.

Microglial lysosomes are larger in high ePRS individuals.

Quantitative analysis of lysosome volume and number per microglia was performed on LAMP1 immunostaining of Iba-1 positive cells in post-mortem human dorsolateral prefrontal cortex tissues. Representative images of two individuals both with high Alzheimer's disease neuropathic change (ADNC 2/3) demonstrating variable LAMP1 signal between low and high ePRS (Figure 3A,B). Mean lysosomal volume and the number of lysosomes present per micron of microglial cell were analyzed while adjusting for age, sex, post-mortem interval and *APOE* genotype. In all cases regardless of AD pathology, and in cases with high AD pathology (Alzheimer disease neuropathic change (ADNC) of 2 and 3 individuals are considered to have sufficient pathology to underlie cognitive decline), high ePRS was significantly associated with larger lysosomal mean volume but not the number of lysosomes (Figure 3C).

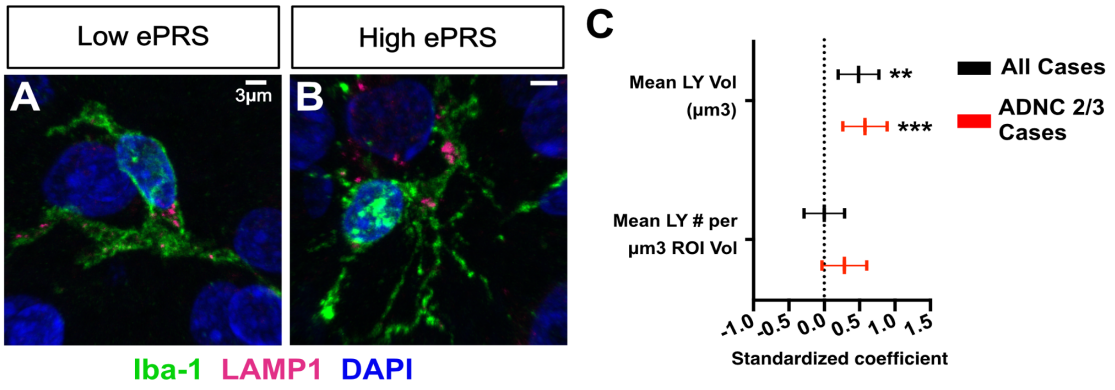

Figure 3:

High ePRS burden increases the volume of lysosomes in post-mortem cortical microglia. A) Representative image of a microglia in an individual with low ePRS and AD pathology. B) Representative image of a microglia with high ePRS and AD pathology. C) High ePRS is correlated with increased mean lysosomal volume in both all cases and individuals with AD pathology. Scale bars are 3um for all images. $^{**}p<0.01$, $^{***}p<0.001$.

Neural nuclei isolated from AD DLPFC tissue demonstrate shared and distinct transcriptomic changes associated with ePRS status

Single-cell/nucleus omics studies of affected AD brain tissue have dramatically improved our understanding of cellular interactions and responses to pathology[32-35]. They serve as platforms for hypothesis generation, enabling exploration of cell type specific pathways and gene networks potentially that may be obscured in bulk tissue RNA sequencing. We performed single nucleus sequencing from 11 low ePRS high ADNC and 12 high ePRS high ADNC DLPFC donors (Table 2). The output of the snRNAseq analysis from the 23 donors demonstrated good representation of all the standard brain cell types (Figure 4A). Across all cell types we observed that the high ePRS cohort showed decreased enrichment of Gene Ontology Biological Processes (GOBP) related to endolysosomal function including macroautophagy and synaptic vesicle acidification, suggesting that increased ELN variant burden may indeed impact endolysosomal function across multiple cell types. Pathways related to protein homeostasis such as protein refolding was similarly depressed in high ePRS donors. Evidence of metabolic changes correlating to ePRS was suggested by depressed electron transport chain and enrichment in glycolysis pathways in select cell types (Figure 4B). These findings identify common alterations in certain endolysosomal pathway metabolic processes and protein processing pathways across all brain cell types associated with higher ePRS risk allele burden. These changes are occurring beyond changes that occur with AD pathology as all individuals in this dataset have AD pathology.

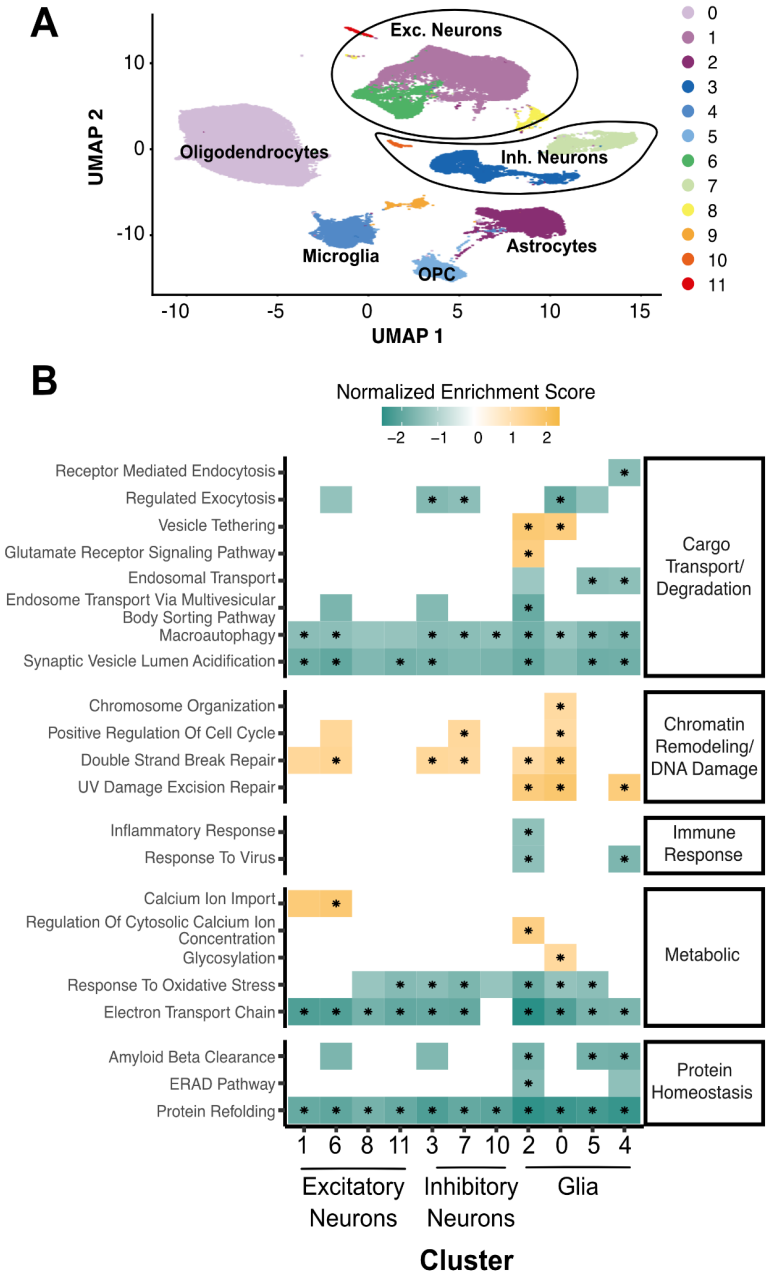

Figure 4:

All cells in high ADNC cases demonstrate shifts in gene expression associated with ePRS risk burden. A) UMAP of the 149,533 nuclei from 23 high ADNC donors (11 low ePRS and 12 high ePRS). B) Pathway analysis of genes shifting expression together in high ePRS individuals versus low ePRS individuals across the different cell types (columns) reveals categories of gene set enrichment sets that were significantly different between high and low ePRS. Some pathways, like chaperone-mediated protein folding, are shifted across cell types while others such as vesicle and DNA-related pathways are more significant in glial populations. Pathways demarcated with a colored square are significant at the $q<0.1$ level while a * indicates that a pathway was significant at $q<0.05$. (OPC oligodendrocyte progenitor cell; Exc. excitatory; Inh. inhibitory).

Neurons: Several excitatory and inhibitory neuronal subtypes across all layers of cortex were identified. The majority of excitatory neurons (clusters 1,6,8,11) were identified to be from layers 4-6 of the cortex[33]. Genes significantly relatively enriched in high ePRS donors in cluster 1 excitatory neurons included kelch like family member 4 (*KLHL4*), and AT-rich interaction domain family 3B (*ARID3B*) transcription factors or DNA-binding proteins involved in cell differentiation and neuronal fate[36, 37]. Genes that regulate neuronal excitability were altered in cluster 1 and in AMPA receptor trafficking to and from the membrane, and ORAI Calcium Release-Activated Calcium Modulator 2 (*ORAI2*) which is part of an inward-rectifying calcium channel[38, 39]. Consistent with these observations, excitatory neurons in cluster 1 and cluster 6 demonstrated enrichment of DNA-repair and calcium ion GOBP gene sets in high ePRS individuals suggesting (Figure 4B**).** These changes in gene sets, rather than just individual genes, indicate that ePRS burden affects broader functional pathways regulating neuronal excitability and cellular resilience. Further, our results suggest that selected neuronal populations differentially regulate their gene expression in different biological function pathways due to ePRS burden.
Inhibitory neurons in our dataset were classified as LAMP5 expressing (cluster 3), parvalbumin/somatostatin expressing (cluster 7) or chandelier neurons (cluster 10). Unlike excitatory neurons, the LAMP5 expressing inhibitory neurons increased the "positive regulation of synaptic transmission glutamatergic" pathway in high ePRS individuals and multiple exocytosis pathways in low ePRS individuals (Fig 4B). Like the LAMP5 expressing inhibitory neurons, the PV/SST neurons also demonstrated significant upregulation of the double strand break repair pathway in high ePRS individuals. In the chandelier neurons, genes that were significantly higher in low ePRS individuals included C1Q/tumor necrosis factor alpha 4 (*C1QTNF4*) and amyloid-beta precursor like protein 1 (*APLP1*) which suggest altered roles in inflammatory and amyloid-beta processing from these neurons. Intriguingly, each of the clusters demonstrated an upregulation of microtubule-associated motor proteins implicating transport pathways in the cells.

Astrocytes: Astrocytes (cluster 2) GSEA analysis demonstrated that many of the representative pathways in each biological category were significantly altered in astrocytes by ePRS risk burden (Figure 4B). These pathways include vesicle tethering and glutamate receptor signaling, as well as cell-cell adhesion which appear to be supported by the individual genes discussed above. Interestingly, pathway analysis also identified pathways involved in DNA repair that are up in high ePRS individuals compared to low ePRS individuals in astrocytes. These findings

suggest that immune response, cell-cell adhesion, metabolism, cargo transport/degradation and DNA repair are processes altered in astrocytes by the increased burden of ePRS risk alleles.

Oligodendrocytes and OPCs: Oligodendrocytes (cluster 0) made up the largest population in our dataset. Gene expression in oligodendrocytes was significantly altered by ePRS, including cysteine-rich protein 2 (*CRIP2*), neurofilament light (*NEFL*), cystatin c (*CST3*), and thymosin beta-10 (*TMSB10*) as down in high ePRS compared to low ePRS individuals all with high ADNC. Additional differentially expressed genes included RAS oncogene family members *RAB39A* and *RAB3A* which are both related to vesicle formation and trafficking[40, 41]; *RAB3A* has been implicated in oligodendrocyte maturation and may participate in myelination programs[41] . Genes that were enriched in high ePRS individuals include fatty acid delta-5 desaturase (*FADS1*). A recent study demonstrated that decreased *FADS1* expression in oligodendrocytes is associated with maintaining cognitive function[42]. Like astrocytes, response to oxidative stress was down while DNA repair and vesicle tethering pathways were up in high ePRS. Interestingly, in contrast to the other glial cells, cell cycle was up in high ePRS individuals, as was chromosome organization and glycosylation.
Oligodendrocytes progenitor cells (OPCs; cluster 5) shared many similarities with their daughter oligodendrocytes, but with some additional shifts associated with ePRS. Amyloid beta clearance and endosomal transport functions were significantly lower in high ePRS individuals in OPCs. Changes in these biological functions differentiate them from the oligodendrocytes, though OPCs in general remain more unaffected by ePRS burden.

Microglia: Microglial cells (cluster 4) demonstrated a less significant shift in individual genes as assessed by pseudobulk measures, based on ePRS. Pathways significantly altered demonstrate a profile similar to astrocytes, with increased UV damage excision repair and decreased response to virus, and amyloid beta clearance in high ePRS individuals (Figure 4B). High ePRS microglia showed relative decrease of enrichment for receptor mediated endocytosis, suggesting that higher ELN burden may alter the regulation of internalization in the context of AD pathology.

In summary, cell type specific transcriptomic data revealed alterations in pathways associated with the ELN that was different between high and low ePRS suggesting that ELN variants may in fact impact ELN function in AD. Additional differentially enriched pathways influenced by ELN

variant load including metabolism, response to DNA damage, chromatin repair and protein degradation may be candidates for further investigation.

ePRS correlates to changes in gene expression changes in ADNC donors across cell types

Pseudobulk DEG analysis, while sound, does not reveal resolution transcriptomic changes at the individual level. The ePRS cohort was originally designed as a binary test between high and low quartiles of ePRS distribution. To ask how ePRS score itself correlates to gene expression, we calculated Pearson's correlation coefficient between donor ePRS and gene expression CPM. Although we had a discontinuous ePRS distribution there were clear transcriptomic associations in multiple cell types with ePRS (Figure 5A). Notably, we identified chromatin remodeling genes in inhibitory neurons such as *CTCF* (Figure 5B) and immune genes including *HMGN2* (Figure 5C) in microglia similar to the pathways and direction of association we found in the GSEA from binary comparison further supporting the notion that ePRS may interact with responses to DNA damage, chromatin remodeling and immune pathways.

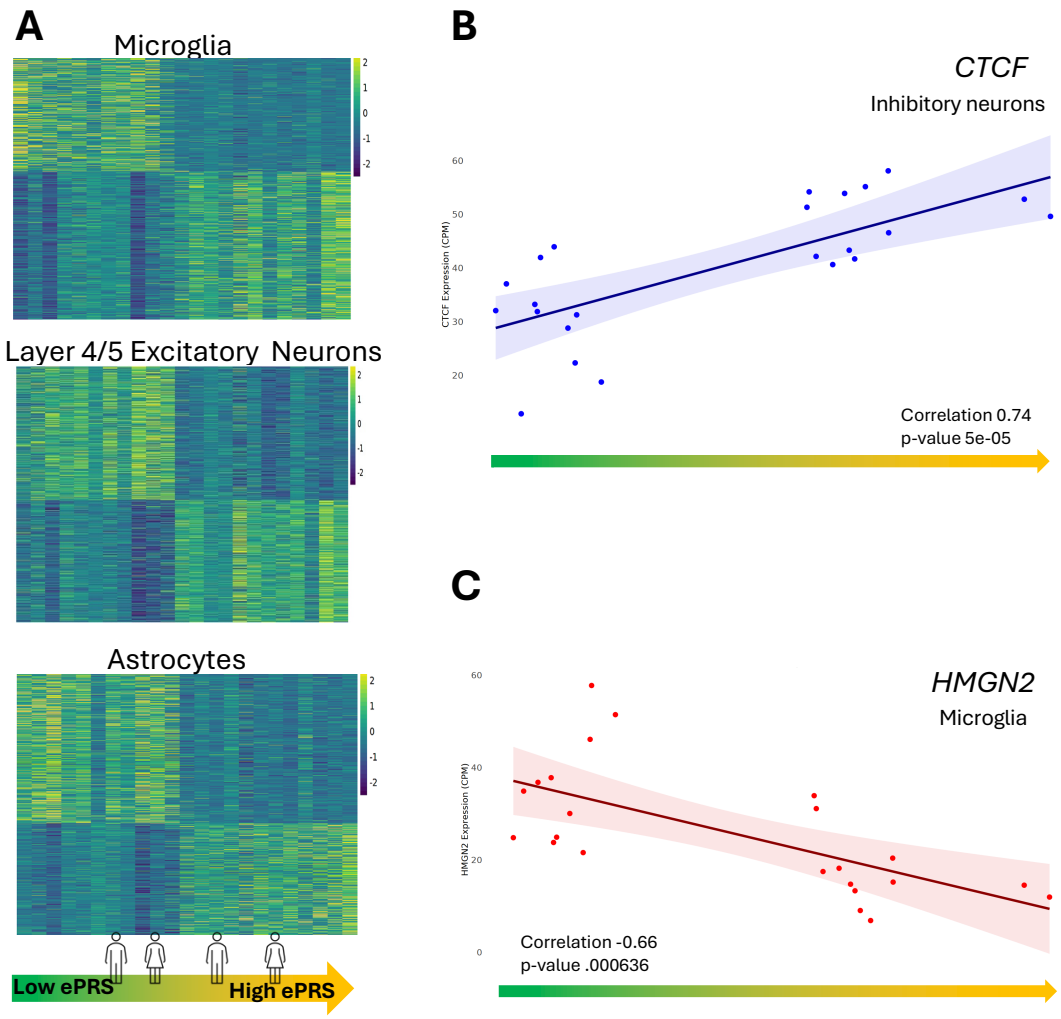

Figure 5:

ePRS correlates to gene expression in neural cell types. A) Heat map displaying gene expression (rows) for each individual (columns) ordered by ePRS demonstrating progressive transcriptomic change with increasing ePRS. On the right, examples of representative gene correlation by scatter plot of B) *CTCF* expression in inhibitory neurons as a function of ePRS and C) *HMGN2* expression in microglia. Pearson's correlation coefficient and p value indicated in figure.

DISCUSSION

In this study we report, to our knowledge the first study in human donor brain tissue, cell type specific molecular and cytopathological features associated with a pathway specific AD polygenic risk score. While PRS have been used for prediction and association with endophenotypes, we show that a targeted, pathway specific PRS can be sensitive to predicting AD diagnosis and pathology. Further, we show that a PRS representing endolysosomal pathway AD risk variants is in fact associated with endolysosomal changes across cell types that is independent of AD pathology. Establishing this association is critical to mapping the molecular effects of AD variants and supporting the premise that variants harboring ELN genes contribute to AD through disruption of the ELN.

ELN cytopathology as an early feature of AD has been well established for years[26]. However, to what degree abnormal endosome and lysosome morphology is simply a secondary consequence of proteopathy progression rather than contributor to the disease process is not fully understood. Despite this, studies in tissue show endosomal pathology in MCI and Down's syndrome subjects prior to the development of amyloid plaques and hiPSC models of AD-related endosome dysfunction similarly show enlarged endosomes in cells that do not yet have much amyloid pathology[26, 29, 43]. The discovery of common AD risk alleles harboring ELN genes and AD rare variants in ELN genes (*SORL1, ABCA7*) provides strong human genetic evidence supporting a pathogenic role for intrinsic changes to ELN function. Here we show that common genetic risk in ELN loci have significant correlations with endo-lysosomal morphology and gene expression in pathways dependent on ELN function, such as autophagy, synaptic function and immune response. Importantly, these changes vary within the diverse cell types of the central nervous system, highlighting both the importance of this pathway for brain homeostasis and the complexity of developing it as a therapeutic target. Our findings of increased numbers, aggregation and enlargement of early endosomes in neurons suggests deficiencies in function of these important organelles. Indeed, other work by our group and others show altered neuronal endosomal function in models lacking key endosomal genes[44, 45]. Importantly, some of the endosomal pathologies we observe are present in low ADNC subjects, further suggesting that they are driven by genetics rather than amyloid pathology.

There are limitations to this study. New loci have emerged in recent AD GWAS, while fine-mapping and colocalization experiments have implicated additional genes at established loci[46]. Genes influence the ELN (ex., *TREM2*[47]) and should be considered as additions to our ePRS.

Several loci have multiple independent signals that may not be adequately captured by the SNPs in our ePRS. For example, while *CLU* rs9331896 and *PTK2B* rs28834970 are often considered the same locus, the two SNPs are not in LD in 1000 Genomes European samples[48, 49]. Confident linking of ELN genes to the tagging SNPs used in GWAS will require additional epigenetic analyses with emerging single cell chromatin accessibility, methylation and 3D chromatin conformation methods.

This study is focused on donors with only high AD pathology and therefore reflects end-stage disease. Ideally, a larger cohort across the spectrum of pathology can provide even further insight into the earlier and later changes that correlate to ELN burden. We attempted to control for secondary effects of AD neurodegenerative processes on the ELN in our assessment of eRPS by conducting high ADNC only comparison across ePRS. Whether by neuropathology or gene expression, we find that despite the same neuropathological burden and diagnosis, higher ePRS appears to drive endolysosomal changes in neurons and microglia.

CONCLUSION

Our work demonstrates that pathway-specific genetic risk scores can reveal biological mechanisms directly relevant to AD pathogenesis. The cell-type specific nature of these changes underscores the complexity of AD and suggests that therapeutic approaches may need to be tailored to address distinct cellular vulnerabilities. For example, neuronal endosomal dysfunction might require different interventions than microglial lysosomal pathology, even though both stem from genetic risk in the endolysosomal network.

The co-occurrence of altered DNA repair pathways with endolysosomal dysfunction across multiple cell types in high ePRS individuals is particularly intriguing. This unexpected finding suggests potential crosstalk between cellular stress responses and endolysosomal function that warrants further investigation. Recent studies have implicated DNA damage in neurodegenerative diseases, and our findings suggest that individuals with high endolysosomal genetic risk may have unique vulnerabilities in maintaining genomic integrity.

Finally, the translational implications of these findings are significant. If pathway-specific genetic risk profiles predict corresponding cellular dysfunctions, this could enable more precise patient stratification for clinical trials and personalized therapeutic approaches. Patients with high endolysosomal genetic risk might benefit most from therapies targeting this pathway, while

others might respond better to interventions addressing alternative mechanisms. Future studies should explore whether interventions targeting endolysosomal function show enhanced efficacy in individuals with high ePRS, potentially advancing the field toward precision medicine for Alzheimer's disease.

METHODS

*Tissues***.** Brain tissue was collected from human donors post-mortem after appropriate consent was obtained during life. All tissues were obtained for processing from the Precision Neuropathology Core at the University of Washington. Cases with diagnoses of non-AD tauopathies, FTLD and ALS were excluded, as well as cases with known genetic chromosomal abnormalities. Additionally, comorbid pathology cortical stroke, history of malignancy, cerebral infection, were exclusionary (Demographic data for each analysis is provided in Tables 2-4 and de-identified individual level data in Supplemental data). All cases had cognitive data available, as well as rigorous neuropathology work-ups in accordance with consensus guidelines[1, 50, 51].

Genotyping

Four mm punches from fresh frozen cerebellum or dorsolateral prefrontal cortex (DLPFC) were lysed and genomic DNA (gDNA) extracted using the GeneJET gDNA Purification Kit (Thermo Scientific #K0722). One microgram of gDNA was sequenced using the Infinium Global Diversity Array 8 v1.0 to detect common single-nucleotide polymorphisms (SNP) and sequenced at the Northwest Genomics Center.

Development and calculation of the ePRS.

Endolysosomal pathway-specific polygenic risk score (ePRS[52]) was developed combining information from 14 AD GWAS SNPs correlated to ELN genes (**Table 1**) using the explained-variance approach[4, 53].

Immunohistochemistry

Immunostaining and IMARIS analysis of endosome and lysosomes. Immunohistochemistry was performed for endosome and lysosome morphology in fresh frozen DLPFC (neuronal endosomes) or paraffin embedded DLPFC (microglia lysosomes) based upon the optimal tissue type for the endolysosomal antibody.

1. *Neuronal endosome morphology analysis from postmortem brain tissue:*

Postmortem brain tissue from 14 low ePRS and 13 high ePRS donors with PMI <8 hours and available fresh frozen inferior parietal lobule tissue were immunolabeled for endosome morphology (Table 2)

Neuron IHC cohort		**Low ePRS** (n = 14)	**High ePRS** (n = 13)
ePRS	Mean +/- SD	8.0 +/- 1.5	15.7 +/- 1.6
Age at death	Mean +/- SD (yrs.)	90.0 +/- 8.1	83.2 +/- 12.4
PMI	Mean +/- SD (hrs.)	4.4 +/- 1.2	6.0 +/- 1.0
Sex	Female % (#)	71% (10)	62% (8)
	Male % (#)	29% (4)	38% (5)
Cognitive status	Normal cognition % (#)	50% (7)	62% (8)
	Dementia % (#)	50% (7)	38% (5)
APOE	E2/E3 % (#)	7% (1)	0% (0)
	E3/E3 % (#)	71% (10)	77% (10)
	E3/E4 % (#)	21% (3)	23% (3)
	E4/E4 % (#)	0% (0)	0% (0)
ADNC	0 % (#)	21% (3)	8% (1)
	1% (#)	17% (1)	23% (3)
	2 % (#)	36% (5)	38% (5)
	3 % (#)	36% (5)	31% (4)

Table 2
Demographics of cohort immunolabeled for neuronal endosomes.

The immunohistochemistry, imaging and image analysis methods used for quantifying early endosome morphology in postmortem brain tissue are described in detail in previously published work[54]. Major steps are described in brief here.

Fresh frozen inferior parietal lobule samples were cut at 5 um thickness and fixed with 4% PFA. Tissue was blocked in 5% normal goat serum (NGS, Jackson ImmunoResearch Laboratories # 005-000-121) + 2.5% bovine serum albumin (BSA, Sigma-Aldrich # A3294) + 0.1% Triton X-100 (Fisher Bioreagents # BP151-100). Primary antibodies used were mouse anti-EEA1(BD Biosciences # 610456) and chicken anti-MAP2 (Abcam # ab92434) diluted 1:500. Secondary antibodies used were goat anti-Chicken IgY (H+L) secondary antibody Alexa Fluor™ 594 (Invitrogen # A11042) and goat anti-Mouse IgG (H+L) Secondary Antibody Alexa Fluor™ 488

(Invitrogen # A11029) diluted 1:1000. Autofluorescence was quenched with TrueBlack (Biotium # 23007) 1:20 according to manufacturer guidelines.

Confocal imaging - Neuron

MAP2-positive pyramidal neurons within the cortical gray matter were imaged on the Leica TCS SP8 confocal microscope with a 63x/1.40 oil lens. Z-stack images were captured in the Leica Application Suite X (LAS X 3.5.5.19976) at 5x zoom with LIGHTNING adaptive deconvolution post-processing, using image acquisition settings as described in previous publication[54]. Total z-size was 1.68 µm with 14 steps and a z-step size of 0.13 µm. An average of ten neurons were imaged per case (range 8-13, due to variability in the size of cortex sampled and proportion of gray matter present).

Image analysis and endosome quantification - Neuron

Endosomal morphology was analyzed from confocal Z-stacks using Bitplane Imaris software (Oxford Instruments). EEA1-positive endosome puncta were identified and segmented in Imaris to quantify the total puncta counts and individual puncta volumes. This quantification was performed within two neuronal regions of interest (ROIs): the MAP2-positive somatodendritic ROI and the perinuclear ROI. The perinuclear ROI boundaries were achieved by expanding a surface from the DAPI-positive nucleus to capture the subpopulation of early endosomes localized most closely with the nucleus.

In order to investigate changes in the early endosome size specifically within the largest subset of early endosomes, we defined an “Enlarged early endosome” subpopulation using the traditional definition of a statistical outlier: early endosomes were considered “Enlarged EEs” if their volume was above 2 standard deviations from the mean volume calculated using ADNC 0-1/low ePRS cases (cases most likely to reflect an early endosome size distribution found in healthy aged controls).

A univariate linear regression model was used to assess relationship between ePRS and early endosome morphology output variables (Mean EE volume, Mean EE # per unit ROI volume, Mean “Enlarged EE” volume, and proportion of “Enlarged EEs” compared to total EE #), and

adjusted for confounding factors age, sex, PMI, and *APOE* genotype. Statistical analyses were performed on the full cohort (n = 27; ADNC low-high cases) as well as an "AD-only" subcohort (n = 19, ADNC intermediate-high cases). The Mann-Whitney test was used for comparison of early endosome morphologies in low versus high ePRS cases and in non-AD versus AD cases.

2. *Microglial lysosome morphology analysis from post-mortem human brain tissue:* Immunohistochemistry of microglia and lysosomal markers was performed on formalin-fixed paraffin embedded tissue from the dorsolateral prefrontal cortex of 13 low ePRS and 13 high ePRS donors (Table 3) following previously published protocols[55] with the addition of the LAMP1 antibody to Iba-1 and DAPI (Lamp-1: Thermo 14-1079-80, 1:250). An Alexa-fluor Donkey anti-Mouse 555 antibody was used for the LAMP1 (ThermoFisher A31570, 1:500).

Microglia IHC cohort		**Low ePRS** (n = 13)	**High ePRS** (n = 13)
ePRS	Mean +/- SD	8.2 +/- 1.6	15.8 +/- 1.6
Age at death	Mean +/- SD (yrs.)	92.5 +/- 5.8	81.5 +/- 11.2
PMI	Mean +/- SD (hrs.)	4.4 +/- 1.3	5.9 +/- 1.6
Sex	Female % (#)	62% (8)	54% (7)
	Male % (#)	38% (5)	46% (6)
Cognitive status	Normal cognition % (#)	62% (8)	54% (7)
	Dementia % (#)	38% (5)	46% (6)
APOE	E2/E3 % (#)	8% (1)	8% (1)
	E3/E3 % (#)	69% (9)	62% (8)
	E3/E4 % (#)	23% (3)	31% (4)
	E4/E4 % (#)	0% (0)	0% (0)
ADNC	0 % (#)	15% (2)	23% (3)
	1 % (#)	8% (1)	8% (1)
	2% (#)	31% (4)	15% (2)
	3 % (#)	38% (5)	38% (5)

Table 3
Demographics of cohort immunolabeled for microglial lysosomes.

Confocal Imaging - Microglia

Slides were imaged using a 40x oil lens on the Leica SP8 laser confocal microscope to create Z-stacks with a step size of 0.47µm, 2.2x zoom, 600 Hz speed, and 1024x1024 format.

Image analysis and lysosome quantification - Microglia

The IMARIS software version 10.1 was used to generate surfaces for Iba-1 using a standardized machine-learning segmentation parameter. The machine-learning parameter was created by selecting the background and foreground across z-stacks. Areas without Iba-1 signal or with noise were selected as background, while areas with Iba-1 signal were selected as foreground. Using the "train and predict" feature, we generated a 3D surface of the Iba-1 signal. Microglia were analyzed if DAPI was fully enclosed in the Iba-1 surface and the whole microglia was present inside the image (no processes cut off by the image edge). When the Iba-1 surface was identified to be less than 7 microns distant from a process, the two surfaces were united. Other background Iba-1 signals were eliminated. The LAMP1 signal contained within the microglial surfaces was identified and surfaces were created for the LAMP1 signal using a similar machine learning approach. For LAMP1, surfaces under 1µm^3 in volume were confirmed to be largely single fluorescent puncta, whereas surfaces larger than 1µm^3 in volume were assessed to be largely dual or clusters of fluorescent puncta. Lysosomes were therefore analyzed in two groups: volumes under 1µm^3, and clusters with volumes between 1 and 15µm^3.

A univariate linear regression model was used to assess relationship between ePRS and lysosome morphology output variables (Mean lysosome volume, Mean lysosome # per unit ROI volume), and adjusted for confounding factors age, sex, PMI, and *APOE* genotype.

<u>Single-nucleus transcriptomic studies</u>

Nuclei isolation and enrichment

For single-nucleus RNA-seq (snRNA-seq), methods largely followed those of Prater, Green et al. (2023). Fresh frozen human DLPFC samples from 11 low ePRS and 12 high ePRS (Table 3) were isolated, as previously described. Briefly, four 2-mm punches of DLPFC gray matter were collected using a biopsy punch (Thermo Fisher Scientific) into a 1.5-ml microcentrifuge tube on dry ice. The nuclei in nuclei suspension solution was layered onto 900 µl of percoll/myelin

gradient buffer[56]. The gradient was centrifuged at 950*g* for 20 min at 4 °C without break and with slow acceleration. The supernatant with myelin were aspirated, and the nuclei pellet was resuspended in resuspension buffer at a concentration of 1,000 nuclei per microliter and proceeded immediately to snRNA-seq. All samples were processed using the 10X Genomics Chromium Next GEM Single Cell 3' Kit v3.1 (#1000268) with a target capture of 10,000 nuclei. Samples were sequenced using either the Illumina NovaSeq 6000 or NovaSeq X platform through the Northwest Genomics Center.

snRNAseq cohort		**Low ePRS** (n = 11)	**High ePRS** (n = 12)
ePRS	Mean +/- SD	8.5 +/- 0.7	16.2 +/- 1.8
Age at death	Mean +/- SD (yrs.)	89.5 +/- 8.0	84.8 +/- 12.5
PMI	Mean +/- SD (hrs.)	4.7 +/- 1.4	6.1 +/- 1.7
Sex	Female % (#)	64% (7)	58% (7)
	Male % (#)	36% (4)	42% (5)
Cognitive status	Normal cognition % (#)	45% (5)	42% (5)
	Dementia % (#)	55% (6)	58% (7)
APOE	E3/E3 % (#)	64% (7)	58% (7)
	E3/E4 % (#)	36% (4)	33% (4)
	E4/E4 % (#)	0% (0)	8% (1)
ADNC	2 % (#)	36% (4)	42% (5)
	3 % (#)	64% (7)	58% (7)

Table 3:

Demographics of snRNAseq cohort.

Alignment, quality control. Methods largely followed those previously published[55]. CellRanger 7.0.2 was used to align the samples using the 2020-A genome provided by 10X Genomics. Analysis was performed in R (R Development Core Team, 2010). Droplets from the samples were combined using Seurat version 4.0.0. The dataset was thresholded to remove droplets containing fewer than 350 genes and droplets with more than 1% mitochondrial reads. Ambient RNA and doublets were detected as previously described[55]. After QC, the total number of nuclei

was 149,533 with 2579.71 average genes/nucleus. A clustering resolution of 0.1 was used after reducing the dimensions of the dataset to 34 principal components

Normalization, Clustering, and Differential Gene Expression testing with GSEA. Analysis proceeded as previously described with noted exceptions[55]: Seurat v4.0.0 was used for all analyses. Harmony was used for batch correction in these datasets. The number of principal components, and clustering resolution selected for each dataset reported are provided in Table 01. For cell type identification in unsorted datasets and prior to subsetting microglia from other cell types after enrichment, marker gene expression from BICCN were used to detect cell types in clusters[33]. All datasets were clustered using the Louvain algorithm with multilevel refinement. GSEA using ClusterProfiler used the 2024 versions of the pathway datasets for GO-BP, Reactome, and Wikipathways.

Correlation of ePRS to cell-type specific gene expression

To identify genes with expression levels correlated with (ePRS) in each cell type, we calculated Pearson correlation coefficients between pseudo-bulk counts per million (CPM) and donor ePRS. Due to variability in cell numbers captured per donor, we applied filtering criteria to donors and genes before correlation analysis. Only genes that were expressed with at least one count in at least one donor were included. Pearson correlation coefficients were computed between gene expression levels and donor ePRS for each cell type. Genes with a correlation coefficient greater than 0.6 and an unadjusted p-value < 0.01 were considered significant.

[1] Montine TJ, Phelps CH, Beach TG, Bigio EH, Cairns NJ, Dickson DW, Duyckaerts C, Frosch MP, Masliah E, Mirra SS, Nelson PT, Schneider JA, Thal DR, Trojanowski JQ, Vinters HV, Hyman BT, National Institute on A, Alzheimer's A: National Institute on Aging-Alzheimer's Association guidelines for the neuropathologic assessment of Alzheimer's disease: a practical approach. Acta Neuropathol 2012, 123:1-11.
[2] Braak H, Braak E: Neuropathological stageing of Alzheimer-related changes. Acta Neuropathol 1991, 82:239-59.
[3] De Strooper B, Karran E: The Cellular Phase of Alzheimer's Disease. Cell 2016, 164:603-15.
[4] Lambert JC, Ibrahim-Verbaas CA, Harold D, Naj AC, Sims R, Bellenguez C, DeStafano AL, Bis JC, Beecham GW, Grenier-Boley B, Russo G, Thorton-Wells TA, Jones N, Smith AV, Chouraki V, Thomas C, Ikram MA, Zelenika D, Vardarajan BN, Kamatani Y, Lin CF, Gerrish A, Schmidt H, Kunkle B, Dunstan ML, Ruiz A, Bihoreau MT, Choi SH, Reitz C, Pasquier F, Cruchaga C, Craig D, Amin N, Berr C, Lopez OL, De Jager PL, Deramecourt V, Johnston JA, Evans D, Lovestone S, Letenneur L, Moron FJ, Rubinsztein DC, Eiriksdottir G, Sleegers K, Goate AM, Fievet N, Huentelman MW, Gill M, Brown K, Kamboh MI, Keller L, Barberger-Gateau P, McGuiness B, Larson EB, Green R, Myers AJ, Dufouil C, Todd S, Wallon D, Love S, Rogaeva E, Gallacher J, St George-Hyslop P, Clarimon J, Lleo A, Bayer A, Tsuang DW, Yu L, Tsolaki M, Bossu P, Spalletta G, Proitsi P, Collinge J, Sorbi S, Sanchez-Garcia F, Fox NC, Hardy J, Deniz Naranjo MC, Bosco P, Clarke R, Brayne C, Galimberti D, Mancuso M, Matthews F, European Alzheimer's Disease I, Genetic, Environmental Risk in Alzheimer's D, Alzheimer's Disease Genetic C, Cohorts for H, Aging Research in Genomic E, Moebus S, Mecocci P, Del Zompo M, Maier W, Hampel H, Pilotto A, Bullido M, Panza F, Caffarra P, Nacmias B, Gilbert JR, Mayhaus M, Lannefelt L, Hakonarson H, Pichler S, Carrasquillo MM, Ingelsson M, Beekly D, Alvarez V, Zou F, Valladares O, Younkin SG, Coto E, Hamilton-Nelson KL, Gu W, Razquin C, Pastor P, Mateo I, Owen MJ, Faber KM, Jonsson PV, Combarros O, O'Donovan MC, Cantwell LB, Soininen H, Blacker D, Mead S, Mosley TH, Jr., Bennett DA, Harris TB, Fratiglioni L, Holmes C, de Bruijn RF, Passmore P, Montine TJ, Bettens K, Rotter JI, Brice A, Morgan K, Foroud TM, Kukull WA, Hannequin D, Powell JF, Nalls MA, Ritchie K, Lunetta KL, Kauwe JS, Boerwinkle E, Riemenschneider M, Boada M, Hiltuenen M, Martin ER, Schmidt R, Rujescu D, Wang LS, Dartigues JF, Mayeux R, Tzourio C, Hofman A, Nothen MM, Graff C, Psaty BM, Jones L, Haines JL, Holmans PA, Lathrop M, Pericak-Vance MA, Launer LJ, Farrer LA, van Duijn CM, Van Broeckhoven C, Moskvina V, Seshadri S, Williams J, Schellenberg GD, Amouyel P: Meta-analysis of 74,046 individuals identifies 11 new susceptibility loci for Alzheimer's disease. Nat Genet 2013, 45:1452-8.
[5] Kunkle BW, Grenier-Boley B, Sims R, Bis JC, Damotte V, Naj AC, Boland A, Vronskaya M, van der Lee SJ, Amlie-Wolf A, Bellenguez C, Frizatti A, Chouraki V, Martin ER, Sleegers K, Badarinarayan N, Jakobsdottir J, Hamilton-Nelson KL, Moreno-Grau S, Olaso R, Raybould R, Chen Y, Kuzma AB, Hiltunen M, Morgan T, Ahmad S, Vardarajan BN, Epelbaum J, Hoffmann P, Boada M, Beecham GW, Garnier JG, Harold D, Fitzpatrick AL, Valladares O, Moutet ML, Gerrish A, Smith AV, Qu L, Bacq D, Denning N, Jian X, Zhao Y, Del Zompo M, Fox NC, Choi SH, Mateo I, Hughes JT, Adams HH, Malamon J, Sanchez-Garcia F, Patel Y, Brody JA, Dombroski BA, Naranjo MCD, Daniilidou M, Eiriksdottir G, Mukherjee S, Wallon D, Uphill J, Aspelund T, Cantwell LB, Garzia F, Galimberti D, Hofer E, Butkiewicz M, Fin B, Scarpini E,

Sarnowski C, Bush WS, Meslage S, Kornhuber J, White CC, Song Y, Barber RC, Engelborghs S, Sordon S, Voijnovic D, Adams PM, Vandenberghe R, Mayhaus M, Cupples LA, Albert MS, De Deyn PP, Gu W, Himali JJ, Beekly D, Squassina A, Hartmann AM, Orellana A, Blacker D, Rodriguez-Rodriguez E, Lovestone S, Garcia ME, Doody RS, Munoz-Fernadez C, Sussams R, Lin H, Fairchild TJ, Benito YA, Holmes C, Karamujic-Comic H, Frosch MP, Thonberg H, Maier W, Roshchupkin G, Ghetti B, Giedraitis V, Kawalia A, Li S, Huebinger RM, Kilander L, Moebus S, Hernandez I, Kamboh MI, Brundin R, Turton J, Yang Q, Katz MJ, Concari L, Lord J, Beiser AS, Keene CD, Helisalmi S, Kloszewska I, Kukull WA, Koivisto AM, Lynch A, Tarraga L, Larson EB, Haapasalo A, Lawlor B, Mosley TH, Lipton RB, Solfrizzi V, Gill M, Longstreth WT, Jr., Montine TJ, Frisardi V, Diez-Fairen M, Rivadeneira F, Petersen RC, Deramecourt V, Alvarez I, Salani F, Ciaramella A, Boerwinkle E, Reiman EM, Fievet N, Rotter JI, Reisch JS, Hanon O, Cupidi C, Andre Uitterlinden AG, Royall DR, Dufouil C, Maletta RG, de Rojas I, Sano M, Brice A, Cecchetti R, George-Hyslop PS, Ritchie K, Tsolaki M, Tsuang DW, Dubois B, Craig D, Wu CK, Soininen H, Avramidou D, Albin RL, Fratiglioni L, Germanou A, Apostolova LG, Keller L, Koutroumani M, Arnold SE, Panza F, Gkatzima O, Asthana S, Hannequin D, Whitehead P, Atwood CS, Caffarra P, Hampel H, Quintela I, Carracedo A, Lannfelt L, Rubinsztein DC, Barnes LL, Pasquier F, Frolich L, Barral S, McGuinness B, Beach TG, Johnston JA, Becker JT, Passmore P, Bigio EH, Schott JM, Bird TD, Warren JD, Boeve BF, Lupton MK, Bowen JD, Proitsi P, Boxer A, Powell JF, Burke JR, Kauwe JSK, Burns JM, Mancuso M, Buxbaum JD, Bonuccelli U, Cairns NJ, McQuillin A, Cao C, Livingston G, Carlson CS, Bass NJ, Carlsson CM, Hardy J, Carney RM, Bras J, Carrasquillo MM, Guerreiro R, Allen M, Chui HC, Fisher E, Masullo C, Crocco EA, DeCarli C, Bisceglio G, Dick M, Ma L, Duara R, Graff-Radford NR, Evans DA, Hodges A, Faber KM, Scherer M, Fallon KB, Riemenschneider M, Fardo DW, Heun R, Farlow MR, Kolsch H, Ferris S, Leber M, Foroud TM, Heuser I, Galasko DR, Giegling I, Gearing M, Hull M, Geschwind DH, Gilbert JR, Morris J, Green RC, Mayo K, Growdon JH, Feulner T, Hamilton RL, Harrell LE, Drichel D, Honig LS, Cushion TD, Huentelman MJ, Hollingworth P, Hulette CM, Hyman BT, Marshall R, Jarvik GP, Meggy A, Abner E, Menzies GE, Jin LW, Leonenko G, Real LM, Jun GR, Baldwin CT, Grozeva D, Karydas A, Russo G, Kaye JA, Kim R, Jessen F, Kowall NW, Vellas B, Kramer JH, Vardy E, LaFerla FM, Jockel KH, Lah JJ, Dichgans M, Leverenz JB, Mann D, Levey AI, Pickering-Brown S, Lieberman AP, Klopp N, Lunetta KL, Wichmann HE, Lyketsos CG, Morgan K, Marson DC, Brown K, Martiniuk F, Medway C, Mash DC, Nothen MM, Masliah E, Hooper NM, McCormick WC, Daniele A, McCurry SM, Bayer A, McDavid AN, Gallacher J, McKee AC, van den Bussche H, Mesulam M, Brayne C, Miller BL, Riedel-Heller S, Miller CA, Miller JW, Al-Chalabi A, Morris JC, Shaw CE, Myers AJ, Wiltfang J, O'Bryant S, Olichney JM, Alvarez V, Parisi JE, Singleton AB, Paulson HL, Collinge J, Perry WR, Mead S, Peskind E, Cribbs DH, Rossor M, Pierce A, Ryan NS, Poon WW, Nacmias B, Potter H, Sorbi S, Quinn JF, Sacchinelli E, Raj A, Spalletta G, Raskind M, Caltagirone C, Bossu P, Orfei MD, Reisberg B, Clarke R, Reitz C, Smith AD, Ringman JM, Warden D, Roberson ED, Wilcock G, Rogaeva E, Bruni AC, Rosen HJ, Gallo M, Rosenberg RN, Ben-Shlomo Y, Sager MA, Mecocci P, Saykin AJ, Pastor P, Cuccaro ML, Vance JM, Schneider JA, Schneider LS, Slifer S, Seeley WW, Smith AG, Sonnen JA, Spina S, Stern RA, Swerdlow RH, Tang M, Tanzi RE, Trojanowski JQ, Troncoso JC, Van Deerlin VM, Van Eldik LJ, Vinters HV, Vonsattel JP, Weintraub S, Welsh-Bohmer KA, Wilhelmsen KC, Williamson J, Wingo TS, Woltjer RL, Wright CB, Yu CE, Yu L, Saba Y, Pilotto A, Bullido MJ, Peters O, Crane PK, Bennett D, Bosco P, Coto

E, Boccardi V, De Jager PL, Lleo A, Warner N, Lopez OL, Ingelsson M, Deloukas P, Cruchaga C, Graff C, Gwilliam R, Fornage M, Goate AM, Sanchez-Juan P, Kehoe PG, Amin N, Ertekin-Taner N, Berr C, Debette S, Love S, Launer LJ, Younkin SG, Dartigues JF, Corcoran C, Ikram MA, Dickson DW, Nicolas G, Campion D, Tschanz J, Schmidt H, Hakonarson H, Clarimon J, Munger R, Schmidt R, Farrer LA, Van Broeckhoven C, M COD, DeStefano AL, Jones L, Haines JL, Deleuze JF, Owen MJ, Gudnason V, Mayeux R, Escott-Price V, Psaty BM, Ramirez A, Wang LS, Ruiz A, van Duijn CM, Holmans PA, Seshadri S, Williams J, Amouyel P, Schellenberg GD, Lambert JC, Pericak-Vance MA, Alzheimer Disease Genetics C, European Alzheimer's Disease I, Cohorts for H, Aging Research in Genomic Epidemiology C, Genetic, Environmental Risk in Ad/Defining Genetic P, Environmental Risk for Alzheimer's Disease C: Genetic meta-analysis of diagnosed Alzheimer's disease identifies new risk loci and implicates Abeta, tau, immunity and lipid processing. Nat Genet 2019, 51:414-30.

[6] Jansen IE, Savage JE, Watanabe K, Bryois J, Williams DM, Steinberg S, Sealock J, Karlsson IK, Hagg S, Athanasiu L, Voyle N, Proitsi P, Witoelar A, Stringer S, Aarsland D, Almdahl IS, Andersen F, Bergh S, Bettella F, Bjornsson S, Braekhus A, Brathen G, de Leeuw C, Desikan RS, Djurovic S, Dumitrescu L, Fladby T, Hohman TJ, Jonsson PV, Kiddle SJ, Rongve A, Saltvedt I, Sando SB, Selbaek G, Shoai M, Skene NG, Snaedal J, Stordal E, Ulstein ID, Wang Y, White LR, Hardy J, Hjerling-Leffler J, Sullivan PF, van der Flier WM, Dobson R, Davis LK, Stefansson H, Stefansson K, Pedersen NL, Ripke S, Andreassen OA, Posthuma D: Genome-wide meta-analysis identifies new loci and functional pathways influencing Alzheimer's disease risk. Nat Genet 2019, 51:404-13.

[7] de Rojas I, Moreno-Grau S, Tesi N, Grenier-Boley B, Andrade V, Jansen IE, Pedersen NL, Stringa N, Zettergren A, Hernandez I, Montrreal L, Antunez C, Antonell A, Tankard RM, Bis JC, Sims R, Bellenguez C, Quintela I, Gonzalez-Perez A, Calero M, Franco-Macias E, Macias J, Blesa R, Cervera-Carles L, Menendez-Gonzalez M, Frank-Garcia A, Royo JL, Moreno F, Huerto Vilas R, Baquero M, Diez-Fairen M, Lage C, Garcia-Madrona S, Garcia-Gonzalez P, Alarcon-Martin E, Valero S, Sotolongo-Grau O, Ullgren A, Naj AC, Lemstra AW, Benaque A, Perez-Cordon A, Benussi A, Rabano A, Padovani A, Squassina A, de Mendonca A, Arias Pastor A, Kok AAL, Meggy A, Pastor AB, Espinosa A, Corma-Gomez A, Martin Montes A, Sanabria A, DeStefano AL, Schneider A, Haapasalo A, Kinhult Stahlbom A, Tybjaerg-Hansen A, Hartmann AM, Spottke A, Corbaton-Anchuelo A, Rongve A, Borroni B, Arosio B, Nacmias B, Nordestgaard BG, Kunkle BW, Charbonnier C, Abdelnour C, Masullo C, Martinez Rodriguez C, Munoz-Fernandez C, Dufouil C, Graff C, Ferreira CB, Chillotti C, Reynolds CA, Fenoglio C, Van Broeckhoven C, Clark C, Pisanu C, Satizabal CL, Holmes C, Buiza-Rueda D, Aarsland D, Rujescu D, Alcolea D, Galimberti D, Wallon D, Seripa D, Grunblatt E, Dardiotis E, Duzel E, Scarpini E, Conti E, Rubino E, Gelpi E, Rodriguez-Rodriguez E, Duron E, Boerwinkle E, Ferri E, Tagliavini F, Kucukali F, Pasquier F, Sanchez-Garcia F, Mangialasche F, Jessen F, Nicolas G, Selbaek G, Ortega G, Chene G, Hadjigeorgiou G, Rossi G, Spalletta G, Giaccone G, Grande G, Binetti G, Papenberg G, Hampel H, Bailly H, Zetterberg H, Soininen H, Karlsson IK, Alvarez I, Appollonio I, Giegling I, Skoog I, Saltvedt I, Rainero I, Rosas Allende I, Hort J, Diehl-Schmid J, Van Dongen J, Vidal JS, Lehtisalo J, Wiltfang J, Thomassen JQ, Kornhuber J, Haines JL, Vogelgsang J, Pineda JA, Fortea J, Popp J, Deckert J, Buerger K, Morgan K, Fliessbach K, Sleegers K, Molina-Porcel L, Kilander L, Weinhold L, Farrer LA, Wang LS, Kleineidam L, Farotti L, Parnetti L, Tremolizzo L, Hausner L, Benussi L, Froelich L, Ikram

MA, Deniz-Naranjo MC, Tsolaki M, Rosende-Roca M, Lowenmark M, Hulsman M, Spallazzi M, Pericak-Vance MA, Esiri M, Bernal Sanchez-Arjona M, Dalmasso MC, Martinez-Larrad MT, Arcaro M, Nothen MM, Fernandez-Fuertes M, Dichgans M, Ingelsson M, Herrmann MJ, Scherer M, Vyhnalek M, Kosmidis MH, Yannakoulia M, Schmid M, Ewers M, Heneka MT, Wagner M, Scamosci M, Kivipelto M, Hiltunen M, Zulaica M, Alegret M, Fornage M, Roberto N, van Schoor NM, Seidu NM, Banaj N, Armstrong NJ, Scarmeas N, Scherbaum N, Goldhardt O, Hanon O, Peters O, Skrobot OA, Quenez O, Lerch O, Bossu P, Caffarra P, Dionigi Rossi P, Sakka P, Mecocci P, Hoffmann P, Holmans PA, Fischer P, Riederer P, Yang Q, Marshall R, Kalaria RN, Mayeux R, Vandenberghe R, Cecchetti R, Ghidoni R, Frikke-Schmidt R, Sorbi S, Hagg S, Engelborghs S, Helisalmi S, Botne Sando S, Kern S, Archetti S, Boschi S, Fostinelli S, Gil S, Mendoza S, Mead S, Ciccone S, Djurovic S, Heilmann-Heimbach S, Riedel-Heller S, Kuulasmaa T, Del Ser T, Lebouvier T, Polak T, Ngandu T, Grimmer T, Bessi V, Escott-Price V, Giedraitis V, Deramecourt V, Maier W, Jian X, Pijnenburg YAL, contributors E, group GAs, consortium D, Igap, consortia P-A, Kehoe PG, Garcia-Ribas G, Sanchez-Juan P, Pastor P, Perez-Tur J, Pinol-Ripoll G, Lopez de Munain A, Garcia-Alberca JM, Bullido MJ, Alvarez V, Lleo A, Real LM, Mir P, Medina M, Scheltens P, Holstege H, Marquie M, Saez ME, Carracedo A, Amouyel P, Schellenberg GD, Williams J, Seshadri S, van Duijn CM, Mather KA, Sanchez-Valle R, Serrano-Rios M, Orellana A, Tarraga L, Blennow K, Huisman M, Andreassen OA, Posthuma D, Clarimon J, Boada M, van der Flier WM, Ramirez A, Lambert JC, van der Lee SJ, Ruiz A: Common variants in Alzheimer's disease and risk stratification by polygenic risk scores. Nat Commun 2021, 12:3417.

[8] Bellenguez Cea: New insights on the genetic etiology of Alzheimer’s and related dementia. medRxiv 2020, doi.org/10.1101/2020.10.0120200659.

[9] Thal DR, Rub U, Orantes M, Braak H: Phases of A beta-deposition in the human brain and its relevance for the development of AD. Neurology 2002, 58:1791-800.

[10] Bellou E, Kim W, Leonenko G, Tao F, Simmonds E, Wu Y, Mattsson-Carlgren N, Hansson O, Nagle MW, Escott-Price V, Alzheimer's Disease Neuroimaging I: Benchmarking Alzheimer's disease prediction: personalised risk assessment using polygenic risk scores across various methodologies and genome-wide studies. Alzheimers Res Ther 2025, 17:6.

[11] Xu Y, Vasiljevic E, Deming YK, Jonaitis EM, Koscik RL, Van Hulle CA, Lu Q, Carboni M, Kollmorgen G, Wild N, Carlsson CM, Johnson SC, Zetterberg H, Blennow K, Engelman CD: Effect of Pathway-Specific Polygenic Risk Scores for Alzheimer's Disease (AD) on Rate of Change in Cognitive Function and AD-Related Biomarkers Among Asymptomatic Individuals. J Alzheimers Dis 2023, 94:1587-605.

[12] Tesi N, van der Lee SJ, Hulsman M, Jansen IE, Stringa N, van Schoor NM, Scheltens P, van der Flier WM, Huisman M, Reinders MJT, Holstege H: Immune response and endocytosis pathways are associated with the resilience against Alzheimer's disease. Transl Psychiatry 2020, 10:332.

[13] Sun Y, Wang M, Zhao Y, Hu K, Liu Y, Liu B, Alzheimer's Disease Neuroimaging I: A Pathway-Specific Polygenic Risk Score Is Associated with Tau Pathology and Cognitive Decline. J Alzheimers Dis 2022, 85:1745-54.

[14] Schork NJ, Elman JA, Alzheimer's Disease Neuroimaging I: Pathway-Specific Polygenic Risk Scores Correlate with Clinical Status and Alzheimer's Disease-Related Biomarkers. J Alzheimers Dis 2023, 95:915-29.

[15] Femminella GD, Harold D, Scott J, Williams J, Edison P, Alzheimer's Disease Neuroimaging I: The Differential Influence of Immune, Endocytotic, and Lipid Metabolism Genes on Amyloid Deposition and Neurodegeneration in Subjects at Risk of Alzheimer's Disease. J Alzheimers Dis 2021, 79:127-39.
[16] Escott-Price V, Myers AJ, Huentelman M, Hardy J: Polygenic risk score analysis of pathologically confirmed Alzheimer disease. Ann Neurol 2017, 82:311-4.
[17] Darst BF, Koscik RL, Racine AM, Oh JM, Krause RA, Carlsson CM, Zetterberg H, Blennow K, Christian BT, Bendlin BB, Okonkwo OC, Hogan KJ, Hermann BP, Sager MA, Asthana S, Johnson SC, Engelman CD: Pathway-Specific Polygenic Risk Scores as Predictors of Amyloid-beta Deposition and Cognitive Function in a Sample at Increased Risk for Alzheimer's Disease. J Alzheimers Dis 2017, 55:473-84.
[18] Ahmad S, Bannister C, van der Lee SJ, Vojinovic D, Adams HHH, Ramirez A, Escott-Price V, Sims R, Baker E, Williams J, Holmans P, Vernooij MW, Ikram MA, Amin N, van Duijn CM: Disentangling the biological pathways involved in early features of Alzheimer's disease in the Rotterdam Study. Alzheimers Dement 2018, 14:848-57.
[19] Karch CM, Goate AM: Alzheimer's disease risk genes and mechanisms of disease pathogenesis. Biol Psychiatry 2015, 77:43-51.
[20] Szabo MP, Mishra S, Knupp A, Young JE: The role of Alzheimer's disease risk genes in endolysosomal pathways. Neurobiol Dis 2022, 162:105576.
[21] Van Acker ZP, Bretou M, Annaert W: Endo-lysosomal dysregulations and late-onset Alzheimer's disease: impact of genetic risk factors. Mol Neurodegener 2019, 14:20.
[22] Young JE, Holstege H, Andersen OM, Petsko GA, Small SA: On the causal role of retromer-dependent endosomal recycling in Alzheimer's disease. Nat Cell Biol 2023, 25:1394-7.
[23] Xue D, Blue EE, Sofer T, Hughes TM, Rotter JI, Fohner AE: Polygenic risk scores for incident dementia in the Multi-Ethnic Study of Atherosclerosis. Genet Epidemiol submitted 2025.
[24] Sleegers K, Bettens K, De Roeck A, Van Cauwenberghe C, Cuyvers E, Verheijen J, Struyfs H, Van Dongen J, Vermeulen S, Engelborghs S, Vandenbulcke M, Vandenberghe R, De Deyn PP, Van Broeckhoven C, consortium B: A 22-single nucleotide polymorphism Alzheimer's disease risk score correlates with family history, onset age, and cerebrospinal fluid Abeta42. Alzheimers Dement 2015, 11:1452-60.
[25] Van Cauwenberghe C, Van Broeckhoven C, Sleegers K: The genetic landscape of Alzheimer disease: clinical implications and perspectives. Genet Med 2016, 18:421-30.
[26] Cataldo AM, Peterhoff CM, Troncoso JC, Gomez-Isla T, Hyman BT, Nixon RA: Endocytic pathway abnormalities precede amyloid beta deposition in sporadic Alzheimer's disease and Down syndrome: differential effects of APOE genotype and presenilin mutations. Am J Pathol 2000, 157:277-86.
[27] Kwart D, Gregg A, Scheckel C, Murphy EA, Paquet D, Duffield M, Fak J, Olsen O, Darnell RB, Tessier-Lavigne M: A Large Panel of Isogenic APP and PSEN1 Mutant Human iPSC Neurons Reveals Shared Endosomal Abnormalities Mediated by APP beta-CTFs, Not Abeta. Neuron 2019, 104:256-70 e5.
[28] Lee JH, Yang DS, Goulbourne CN, Im E, Stavrides P, Pensalfini A, Chan H, Bouchet-Marquis C, Bleiwas C, Berg MJ, Huo C, Peddy J, Pawlik M, Levy E, Rao M, Staufenbiel M, Nixon

RA: Faulty autolysosome acidification in Alzheimer's disease mouse models induces autophagic build-up of Abeta in neurons, yielding senile plaques. Nat Neurosci 2022, 25:688-701.
[29] Knupp A, Mishra S, Martinez R, Braggin JE, Szabo M, Kinoshita C, Hailey DW, Small SA, Jayadev S, Young JE: Depletion of the AD Risk Gene SORL1 Selectively Impairs Neuronal Endosomal Traffic Independent of Amyloidogenic APP Processing. Cell Rep 2020, 31:107719.
[30] Filippone A, Pratico D: Endosome Dysregulation in Down Syndrome: A Potential Contributor to Alzheimer Disease Pathology. Ann Neurol 2021, 90:4-14.
[31] Somogyi A, Kirkham ED, Lloyd-Evans E, Winston J, Allen ND, Mackrill JJ, Anderson KE, Hawkins PT, Gardiner SE, Waller-Evans H, Sims R, Boland B, O'Neill C: The synthetic TRPML1 agonist ML-SA1 rescues Alzheimer-related alterations of the endosomal-autophagic-lysosomal system. J Cell Sci 2023, 136.
[32] Lee H, Aylward AJ, Pearse RV, 2nd, Lish AM, Hsieh YC, Augur ZM, Benoit CR, Chou V, Knupp A, Pan C, Goberdhan S, Duong DM, Seyfried NT, Bennett DA, Taga MF, Huynh K, Arnold M, Meikle PJ, De Jager PL, Menon V, Young JE, Young-Pearse TL: Cell-type-specific regulation of APOE and CLU levels in human neurons by the Alzheimer's disease risk gene SORL1. Cell Rep 2023, 42:112994.
[33] Emani PS, Liu JJ, Clarke D, Jensen M, Warrell J, Gupta C, Meng R, Lee CY, Xu S, Dursun C, Lou S, Chen Y, Chu Z, Galeev T, Hwang A, Li Y, Ni P, Zhou X, Psych ECd, Bakken TE, Bendl J, Bicks L, Chatterjee T, Cheng L, Cheng Y, Dai Y, Duan Z, Flaherty M, Fullard JF, Gancz M, Garrido-Martin D, Gaynor-Gillett S, Grundman J, Hawken N, Henry E, Hoffman GE, Huang A, Jiang Y, Jin T, Jorstad NL, Kawaguchi R, Khullar S, Liu J, Liu J, Liu S, Ma S, Margolis M, Mazariegos S, Moore J, Moran JR, Nguyen E, Phalke N, Pjanic M, Pratt H, Quintero D, Rajagopalan AS, Riesenmy TR, Shedd N, Shi M, Spector M, Terwilliger R, Travaglini KJ, Wamsley B, Wang G, Xia Y, Xiao S, Yang AC, Zheng S, Gandal MJ, Lee D, Lein ES, Roussos P, Sestan N, Weng Z, White KP, Won H, Girgenti MJ, Zhang J, Wang D, Geschwind D, Gerstein M, Psych EC: Single-cell genomics and regulatory networks for 388 human brains. Science 2024, 384:eadi5199.
[34] Mathys H, Boix CA, Akay LA, Xia Z, Davila-Velderrain J, Ng AP, Jiang X, Abdelhady G, Galani K, Mantero J, Band N, James BT, Babu S, Galiana-Melendez F, Louderback K, Prokopenko D, Tanzi RE, Bennett DA, Tsai LH, Kellis M: Single-cell multiregion dissection of Alzheimer's disease. Nature 2024, 632:858-68.
[35] Mathys H, Davila-Velderrain J, Peng Z, Gao F, Mohammadi S, Young JZ, Menon M, He L, Abdurrob F, Jiang X, Martorell AJ, Ransohoff RM, Hafler BP, Bennett DA, Kellis M, Tsai LH: Single-cell transcriptomic analysis of Alzheimer's disease. Nature 2019, 570:332-7.
[36] Patsialou A, Wilsker D, Moran E: DNA-binding properties of ARID family proteins. Nucleic Acids Res 2005, 33:66-80.
[37] Asmar AJ, Abrams SR, Hsin J, Collins JC, Yazejian RM, Wu Y, Cho J, Doyle AD, Cinthala S, Simon M, van Jaarsveld RH, Beck DB, Kerosuo L, Werner A: A ubiquitin-based effector-to-inhibitor switch coordinates early brain, craniofacial, and skin development. Nat Commun 2023, 14:4499.

[38] Yoast RE, Emrich SM, Zhang X, Xin P, Johnson MT, Fike AJ, Walter V, Hempel N, Yule DI, Sneyd J, Gill DL, Trebak M: The native ORAI channel trio underlies the diversity of Ca(2+) signaling events. Nat Commun 2020, 11:2444.
[39] Gu X, Mao X, Lussier MP, Hutchison MA, Zhou L, Hamra FK, Roche KW, Lu W: GSG1L suppresses AMPA receptor-mediated synaptic transmission and uniquely modulates AMPA receptor kinetics in hippocampal neurons. Nat Commun 2016, 7:10873.
[40] Jordan KL, Koss DJ, Outeiro TF, Giorgini F: Therapeutic Targeting of Rab GTPases: Relevance for Alzheimer's Disease. Biomedicines 2022, 10.
[41] Anitei M, Cowan AE, Pfeiffer SE, Bansal R: Role for Rab3a in oligodendrocyte morphological differentiation. J Neurosci Res 2009, 87:342-52.
[42] Wu X, Jiang L, Qi H, Hu C, Jia X, Lin H, Wang S, Lin L, Zhang Y, Zheng R, Li M, Wang T, Zhao Z, Xu M, Xu Y, Chen Y, Zheng J, Bi Y, Lu J: Brain tissue- and cell type-specific eQTL Mendelian randomization reveals efficacy of FADS1 and FADS2 on cognitive function. Transl Psychiatry 2024, 14:77.
[43] Hung C, Tuck E, Stubbs V, van der Lee SJ, Aalfs C, van Spaendonk R, Scheltens P, Hardy J, Holstege H, Livesey FJ: SORL1 deficiency in human excitatory neurons causes APP-dependent defects in the endolysosome-autophagy network. Cell Rep 2021, 35:109259.
[44] Saha O, Melo de Farias AR, Pelletier A, Siedlecki-Wullich D, Landeira BS, Gadaut J, Carrier A, Vreulx AC, Guyot K, Shen Y, Bonnefond A, Amouyel P, Tcw J, Kilinc D, Queiroz CM, Delahaye F, Lambert JC, Costa MR: The Alzheimer's disease risk gene BIN1 regulates activity-dependent gene expression in human-induced glutamatergic neurons. Mol Psychiatry 2024, 29:2634-46.
[45] Mishra S, Knupp A, Szabo MP, Williams CA, Kinoshita C, Hailey DW, Wang Y, Andersen OM, Young JE: The Alzheimer's gene SORL1 is a regulator of endosomal traffic and recycling in human neurons. Cell Mol Life Sci 2022, 79:162.
[46] Lee WP, Choi SH, Shea MG, Cheng PL, Dombroski BA, Pitsillides AN, Heard-Costa NL, Wang H, Bulekova K, Kuzma AB, Leung YY, Farrell JJ, Lin H, Naj A, Blue EE, Nusetor F, Wang D, Boerwinkle E, Bush WS, Zhang X, De Jager PL, Dupuis J, Farrer LA, Fornage M, Martin E, Pericak-Vance M, Seshadri S, Wijsman EM, Wang LS, Schellenberg GD, Destefano AL, Haines JL, Peloso GM: Association of Common and Rare Variants with Alzheimer's Disease in over 13,000 Diverse Individuals with Whole-Genome Sequencing from the Alzheimer's Disease Sequencing Project. medRxiv 2023.
[47] Filipello F, You SF, Mirfakhar FS, Mahali S, Bollman B, Acquarone M, Korvatska O, Marsh JA, Sivaraman A, Martinez R, Cantoni C, De Feo L, Ghezzi L, Minaya MA, Renganathan A, Cashikar AG, Satoh JI, Beatty W, Iyer AK, Cella M, Raskind WH, Piccio L, Karch CM: Defects in lysosomal function and lipid metabolism in human microglia harboring a TREM2 loss of function mutation. Acta Neuropathol 2023, 145:749-72.
[48] Genomes Project C, Auton A, Brooks LD, Durbin RM, Garrison EP, Kang HM, Korbel JO, Marchini JL, McCarthy S, McVean GA, Abecasis GR: A global reference for human genetic variation. Nature 2015, 526:68-74.
[49] Machiela MJ, Chanock SJ: LDlink: a web-based application for exploring population-specific haplotype structure and linking correlated alleles of possible functional variants. Bioinformatics 2015, 31:3555-7.

[50] Nelson PT, Lee EB, Cykowski MD, Alafuzoff I, Arfanakis K, Attems J, Brayne C, Corrada MM, Dugger BN, Flanagan ME, Ghetti B, Grinberg LT, Grossman M, Grothe MJ, Halliday GM, Hasegawa M, Hokkanen SRK, Hunter S, Jellinger K, Kawas CH, Keene CD, Kouri N, Kovacs GG, Leverenz JB, Latimer CS, Mackenzie IR, Mao Q, McAleese KE, Merrick R, Montine TJ, Murray ME, Myllykangas L, Nag S, Neltner JH, Newell KL, Rissman RA, Saito Y, Sajjadi SA, Schwetye KE, Teich AF, Thal DR, Tome SO, Troncoso JC, Wang SJ, White CL, 3rd, Wisniewski T, Yang HS, Schneider JA, Dickson DW, Neumann M: LATE-NC staging in routine neuropathologic diagnosis: an update. Acta Neuropathol 2023, 145:159-73.
[51] Latimer CS, Melief EJ, Ariza-Torres J, Howard K, Keen AR, Keene LM, Schantz AM, Sytsma TM, Wilson AM, Grabowski TJ, Darvas M, O'Connor KD, Nolan AL, Edlow BL, Mac Donald CL, Keene CD: Protocol for the Systematic Fixation, Circuit-Based Sampling, and Qualitative and Quantitative Neuropathological Analysis of Human Brain Tissue. Methods Mol Biol 2023, 2561:3-30.
[52] Strohbehn SD: Examining the Association Between an Endolysosomal Polygenic Risk Score and Alzheimer's Disease. Institute for Public Health Genetics. Seattle, WA: University of Washington, 2023. p. 74.
[53] Che R, Motsinger-Reif AA: A new explained-variance based genetic risk score for predictive modeling of disease risk. Stat Appl Genet Mol Biol 2012, 11:Article 15.
[54] Rose SE, Williams CA, Hailey DW, Mishra S, Kirkland A, Keene CD, Garden GA, Jayadev S, Young JE: Advancements in high-resolution 3D microscopy analysis of endosomal morphology in postmortem Alzheimer's disease brains. Front Neurosci 2023, 17:1321680.
[55] Prater KE, Green KJ, Mamde S, Sun W, Cochoit A, Smith CL, Chiou KL, Heath L, Rose SE, Wiley J, Keene CD, Kwon RY, Snyder-Mackler N, Blue EE, Logsdon B, Young JE, Shojaie A, Garden GA, Jayadev S: Human microglia show unique transcriptional changes in Alzheimer's disease. Nat Aging 2023.
[56] de Groot CJ, Hulshof S, Hoozemans JJ, Veerhuis R: Establishment of microglial cell cultures derived from postmortem human adult brain tissue: immunophenotypical and functional characterization. Microsc Res Tech 2001, 54:34-9.